

POLYNOMIAL TRAJECTORY PREDICTIONS FOR IMPROVED LEARNING PERFORMANCE

Ido Freeman, Kun Zhao

Aptiv Services Deutschland GmbH
Wuppertal, Germany
<first name>.<surname>@aptiv.com

Anton Kummert

University of Wuppertal, Germany
kummert@uni-wuppertal.de

ABSTRACT

The rising demand for Active Safety systems in automotive applications stresses the need for a reliable short to mid-term trajectory prediction. Anticipating the unfolding path of road users, one can act to increase the overall safety. In this work, we propose to train artificial neural networks for movement understanding by predicting trajectories in their natural form, as a function of time. Predicting polynomial coefficients allows us to increased accuracy and improve generalisation.

Index Terms— active safety, trajectory prediction, motion understanding, autonomous driving.

1. INTRODUCTION

Reliably predicting the future movement of road users will positively affect road safety, not only in completely autonomous applications but also in current features such as Autonomous Emergency Braking (AEB) or Adaptive Cruise Control (ACC).

Traditionally, there has been an emphasis on detection and recognition, with algorithms like MaskRCNN [1] showing a good combination of accuracy and efficiency. However, detection is not enough for a fully functional system. Considering the example of an ACC system, the detection and classification are merely the first steps in the pipeline. An ACC system which anticipates its neighbours' movements is able to better prepare for events like cut-ins or sudden breaking.

As with other tasks, this one was also enabled by public datasets like the well studied NGSim dataset [2] and the more recent, but with restrictive terms of use, HighD dataset [3]. While real-world data is very credible, it should also be used with care as it often features strong biases like region and sparsity. As an example, [4] demonstrated near state-of-the-art results on NGSim with a rather simple Kalman constant velocity model.

Across the different works, one can see that the community tends to agree on the general framework for trajectory prediction. Some, like [5], use Generative Adversarial

Networks (GANs), others, like [6], use Variational Auto-Encoders (VAEs). There are also multiple ways to handle attention [[7], [5], [8]]. Yet, the general structure of an encoder-attention-decoder model remains the same. Furthermore, the decoder is predicting a series of coordinates, representing the future spatial positions of an agent. The predicted series of offsets is constant and gets hard-coded into the model during training.

Although certainly convenient, the predetermined temporal offsets have two drawbacks. First, they do not impose any sort of temporal consistency. Trajectories jagged around the ground truth could potentially result in undesired side effects. Predicting cut-in events, for example, such jitters around a lane marking would mean multiple intersection points, turning a predicted cut-in event into a small set of possible cut-ins and thus reducing reliability. Second, the prediction resolution of the fixed offsets is limiting. Certain scenarios, e.g. congested traffic, require a rather high prediction resolution while others, e.g. a clear motorway, are less sensitive.

In this work, we propose a novel framework for continuous trajectory training and prediction with artificial neural networks. Our main contributions are:

- An alternative output formulation for trajectory prediction which better matches the nature of movement.
- An adjustment to the common uncertainty propagation to allow for a continuous variance estimation.
- A novel training scheme for enhanced generalisation.

2. RELATED WORK

One of the first works in the field dates back to 1995, with Helbing et al. proposing a model for pedestrian dynamics [9] which defines attractive and retractive forces between pedestrians. A statistical approach for behaviour prediction in a multi-agent environment was proposed by [10] and followed by [11] which proposed a Kalman filter based approach.

More recent works mostly focus on environment understanding and the plurality of possible futures, i.e. multimodality. The former is represented by works as [12] and [13] which proposed social pooling for multi-agent integration. ChauffeurNet [14] modelled the environment as binary pixel masks which are convolved as an image. Finally, projects such as [15] train end-to-end systems for steering decisions.

A slightly different strain of work looks into kinematic constraints. Instead of learning the well studied rules of physics from data, they are directly built into the network by design, reducing the prediction to its variable parts. A good overview is provided by [16], while [17] has more recently modelled vehicle movement using the bicycle model while predicting the acceleration and the steering angle.

This work proposes a loose variant of the latter class of works. Instead of a kinematic model, and similar to [18], we predict continuous functions. Trained with our random anchoring scheme, we improve generalisation while being more accurate and flexible comparing to coordinates prediction.

Using neural networks for polynomial coefficients was discussed before. In 2014, Andoni et al. predicted sparse polynomials with increased robustness using neural networks [19]. More recently [20] used polynomials for optical flow and video stabilisation. Finally, [21] incorporated the polynomials into their very network structure. Their non-linearity polynomials in their generative model lead to appealing results on a wide variety of tasks.

3. POLYNOMIAL PREDICTION FRAMEWORK

Our framework consists of three parts. The position prediction, the variance estimation and the training scheme. This section discusses and explains these in detail.

3.1. Position Prediction

Assuming an arbitrary neural network $f(\cdot)$ which takes in a time series of states (S) of an arbitrary length, with $i \in \mathbb{N}$ different agents including the ego vehicle. The goal is to predict the trajectories of all agents for the following T frames, with t_0 being the current time step.

To neutralise the fixed coordinate system, we use position increments, defining $[\delta x_t^i, \delta y_t^i] = [x_t^i, y_t^i] - [x_{t-1}^i, y_{t-1}^i]$. Each state is defined as $s_t^i \in S = [\delta x_t^i, \delta y_t^i, v_t^i, \alpha_t^i, \theta_t^i, l_{2t}^i, \varphi_t^i]$. I.e., position increments, current velocity, acceleration, heading angle and, finally, the polar coordinates to the ego agent, respectively. Prior art defines the output of such a network as

$$f(I) = [x_1, y_1, x_2, y_2, \dots, x_T, y_T]. \quad (1)$$

The origin of this coordinate system is the ego vehicle at the current t_0 . We define our model's output as

$$f(I) = \{a_1, \dots, a_{d_x}, b_1, \dots, b_{d_y}\} = \{A \cup B\}. \quad (2)$$

Meaning that our neural network predicts two sets of parameters $A = \{a_1, \dots, a_{d_x}\}$ and $B = \{b_1, \dots, b_{d_y}\}$. These parameterise two polynomial functions, $x(t)$ and $y(t)$, which describe the trajectory along the time dimension. The polynomial form for $x(t)$ is

$$x(t) = \sum_{j=1}^{d_x} a_j * t^j \quad (3)$$

The definition of $y(t)$ is analogous. The polynomials might have different degrees. Furthermore, the 0^{th} coefficient is ignored since it represents the bias on the current position which is, by definition, the origin.

3.2. Variance Estimation

Joint position and variance prediction, as discussed in [12] and [22], is now a standard. Yet as we do not have predefined prediction points but would still like to get the uncertainty of the predicted trajectories, we have to adjust the formulation.

3.2.1. Variance with Polynomials

Predicting polynomial coefficients renders the formulation of [22] inapplicable. Here, the network's outputs the polynomial coefficients $\{a_1, \dots, a_{d_x}\}$ along their respective standard deviations $\{\sigma_{a_1}, \dots, \sigma_{a_{d_x}}\}$. Since the loss is evaluated by sampling from the position polynomials, we need to propagate the coefficient variances to a positional variance form.

With the same assumptions as in [12], the respective covariance matrix $cov(A)$ is denoted as

$$cov(A) = \begin{pmatrix} \sigma_{a_1}^2 & 0 & \dots & 0 \\ 0 & \sigma_{a_2}^2 & \dots & 0 \\ \dots & \dots & \dots & 0 \\ 0 & 0 & 0 & \sigma_{a_{d_x}}^2 \end{pmatrix}. \quad (4)$$

In Equation 3, $x(t)$ is a linear combination of polynomial coefficients a_j . Given the covariance $cov(A)$, the variance of function $x(t)$ at time frame t is

$$var(x(t)) = \sum_{j=1}^{d_x} \sigma_j^2 * (t^j)^2. \quad (5)$$

The probability density function is then

$$P(x(t)) = \frac{\exp(-\frac{1}{2}(x(t) - \mu_{x,t})^\top var(x(t))^{-1}(x(t) - \mu_{x,t}))}{\sqrt{(2\pi)^{d_x} |var(x(t))|}}. \quad (6)$$

$|\text{var}(x(t))|$ is the determinant of $\text{cov}(x(t))$. $\mu_{x,t}$ is the ground truth observation for the lateral axis at time t . Finally, the negative log probability is used as a loss and, surely enough, the term for $y(t)$ follows analogously.

3.3. Training Scheme

Our definition of the output layers also allows for an improved training scheme. Evaluating the predictions for a series of temporal offsets means a simple vector-matrix multiplication and results in a series of coordinates.

Nevertheless, training a high order, non-linear function on a small number of fixed offsets is the textbook example of overfitting. As discussed in Section 4, when trained with two fixed anchors (coordinates at fixed offsets), the model strongly overfits the desired offsets. We improve this by introducing two adjustments to the training scheme. First, we increase the number of anchor points, i.e. the evaluated coordinates based on which the loss is calculated. This is a common practice with coordinates for a higher prediction resolution. Second, instead of fixed temporal offsets, e.g. predicting future frames $[5, 10, 15, \dots]$, we define a uniform distribution over an offset range $\mathcal{U}\{\min \in \mathbb{N}, \max \in \mathbb{N}\}$. For each sample during training, an offset r is drawn from this distribution while all other anchor points are evenly spread accordingly.

$$[t_1, t_2, \dots, t_T] = [\lfloor r * \frac{1}{T} \rfloor, \lfloor r * \frac{2}{T} \rfloor, \dots, \lfloor r * \frac{T}{T} \rfloor]. \quad (7)$$

For example, for 4 anchors from the integer range of $\mathcal{U}\{5, 30\}$ frames, the variate $r = 20$ is drawn. The loss is calculated based on the following frame offsets $[t_1, t_2, t_3, t_4] = [5, 10, 15, 20]$. Non-integer frame indices are floored. Notice that the lower range is hence over-represented while the upper range becomes less frequent. To reduce this over-representation, the lower boundary of the range is set in practice to a rather large number while the upper boundary is set to be a bit larger than the maximal desired prediction offset. In the final system with a prediction range of 50 frames, the uniform distribution is set to $\mathcal{U}\{35, 55\}$.

4. EXPERIMENTS

Since our main aim throughout the experiments was to test the limits and performance of our polynomial predictions, all experiments were done with a simple Gated Recurrent Units (GRU) [23] based encoder-attention-decoder architecture. It consists of a two-layer encoder and a three-layer decoder while the attention is based on [24]. All layers have 32 units and use the default Keras GRU implementation.

Using multimodal architectures, we have established that modality selection, i.e. which of the modalities to use for evaluation, quickly become the bottleneck. That is, the

problem of modality prediction is exchanged for the problem of modality selection for testing. As multimodality is not the focus of this work, we opted out to the model of [13] where the decoder is conditioned on the modality label, both in testing and training.

Due to its free licence, we used the NGSim dataset [2]. It consists of two main motorway segments in the USA which were recorded by static traffic cameras at 10Hz and three different times of day (dawn, midday, dusk). The tracks are divided into segments of 200 frames and temporarily split into train and test sets with a 3 : 1 ratio. Due to the relatively small dataset, we refrained from extracting validation data. The training set was then filtered to half the amount of constant velocity, straight driving tracks, leaving us with ~ 7500 training samples and ~ 3400 testing samples. Furthermore, we always predict from the first to the last frame, i.e. no "warm-up phase" for the GRU. All results in this section are given in Average Displacement Error (ADE) in metres, i.e. lower is better. Time is given in seconds.

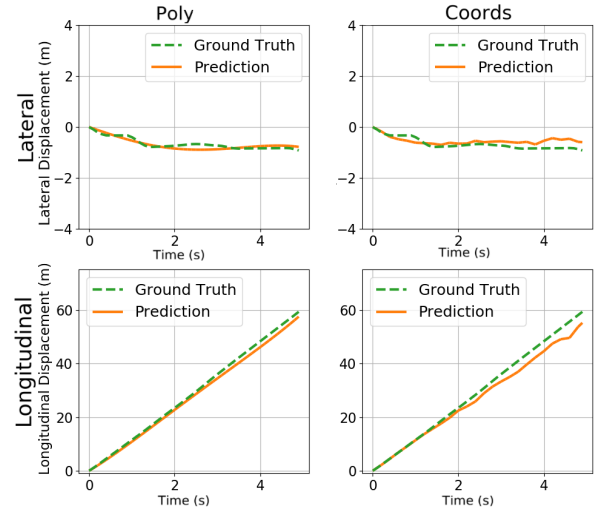


Fig. 1: Axis-wise visualisation of the predictions. Right: coordinates prediction. Left: our polynomial prediction. The top and bottom rows are for the lateral and longitudinal axes, respectively.

4.1. Visual Evaluation

Both architectures are capable of producing visually appealing result. However, taking a closer look at the results (Figure 1), one can see the inconsistencies of the coordinates model. We explain this with two known properties of neural networks - overfitting and prediction resolution.

During training, the network learns to overfit its prediction offsets, subsequently harming its generalisation capacity. Additionally, as noticed by works like [25], neural networks can reliably regress values, but only to a certain precision.

Offset (sec)	Coords baseline	Poly (ours)	CS-LSTM (M) [13]	MFP-1 [26]
1	0.43	0.55	0.62	0.54
2	1.00	0.93	1.27	1.16
3	1.72	1.64	2.09	1.90
4	2.76	2.64	3.10	2.78
5	3.98	3.85	4.37	3.83

Table 1: The RMSE results (in metres) of coordinates vs. polynomial training. For reference, two other SotA results are provided.

4.2. Quantifiable Evaluation

We further compare our model’s performance to coordinates prediction at five consecutive seconds. The results are presented in Table 1 along with two other works for a reference.

In a further experiment, we train both output types with both 5 and 25 anchor points. The results, shown in Figure 2 (right), are quite interesting. Looking at the 5 anchors models and the 25 anchors models separately, one can see favourable performance of the polynomial models starting at around 1.5 seconds. However, even between both types of models a clear improvement is visible, supporting our claim that models better generalise with the increasing number of anchors.

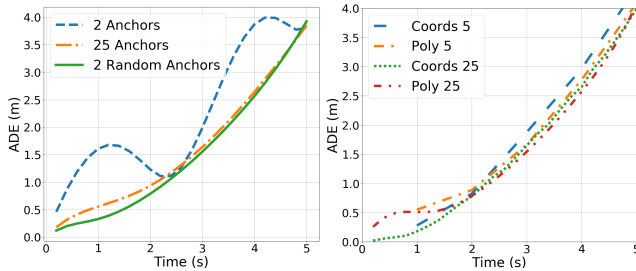


Fig. 2: Left: evaluating our random anchoring. Even with as little as 2 anchors the polynomial accuracies exceed the 25 fixed anchors. Right: the results with 5 and 25 anchors per trajectory. For a given number of anchors, the polynomial prediction models outperform the classical coordinates.

4.3. Random Anchoring

We claim that when training on a fixed set of predetermined temporal offsets the network only regards these few coordinates, thus learning less about the movement as a whole. As coordinates are fixed by definition, we test using our more flexible polynomials. The first model is trained using two anchors at $t_0 + 25$ and $t_0 + 50$ frames. The second model is trained on 25 evenly spread frames, i.e. $[2, 4, 6, \dots, 48, 50]$.

The third model is trained with two random anchors as described in Section 3.3.

The results are visualised in Figure 2 (left). Even with as little as two random labels per sample, the network manages to overcome the extreme overfitting seen in the baseline and generalise better.

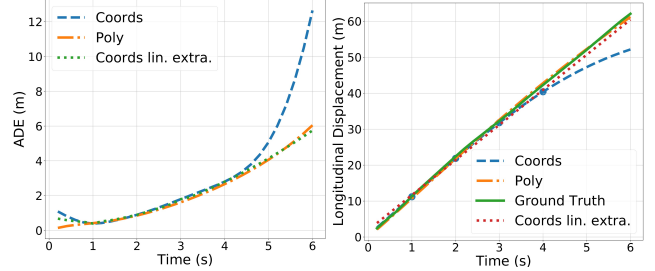


Fig. 3: Left: the ADE curve for the extrapolation experiment. Right: an example of an extrapolated longitudinal trajectory.

4.4. Extrapolation

To further test generalisation capacities, we studied the extrapolation to unseen time steps.

Both networks were trained on four seconds with four anchor points and evaluate them on a six seconds time span. The results are evaluated at five frames per second, i.e., a 0.2 seconds resolution. For the coordinates extrapolation, we used NumPy’s *polyfit* function and fit both a linear curve and one of the same order as our polynomials.

The results for the entire test set are shown in Figure 3 (left). For the same polynomial degree our predictions better extend to new horizons. Yet it seems that the linear extrapolation of the coordinates prediction does similarly well. We use Figure 3 (right) as an example to explain this and show that often a simple linear interpolation performs well on average, especially on a dataset which mostly includes straight trajectories.

5. LIMITATIONS

Even though our polynomial trajectories better match the ground truth predictions, we have noticed some limitations. For one, pedestrians typically require a higher degree of freedom than our polynomials enable, e.g. walking, stopping for a bit and then continuing to walk. Second, as seen in Figure 1, minor movements inside the lane are hard to represent. We do claim however that such cruising artefacts are not very relevant for active safety applications.

6. CONCLUSIONS

We presented a novel framework for polynomial trajectories with artificial neural networks. With the rather general

constraint of continuity our framework improves the generalisation of predicted trajectories. Our lightweight framework is easy to implement using the common deep learning frameworks and is not limited to a specific architecture.

References

- [1] Kaiming He et al., “Mask r-cnn,” in *Proceedings of the IEEE international conference on computer vision*, 2017, pp. 2961–2969.
- [2] US Department of Transportation, “Ngsimnext generation simulation,” 2006.
- [3] Robert Krajewski et al., “The highd dataset: A drone dataset of naturalistic vehicle trajectories on german highways for validation of highly automated driving systems,” in *2018 21st International Conference on Intelligent Transportation Systems (ITSC)*, 2018, pp. 2118–2125.
- [4] Jean Mercat et al., “Inertial single vehicle trajectory prediction baselines and applications with the ngsim dataset,” *arXiv preprint arXiv:1908.11472*, 2019.
- [5] Agrim Gupta et al., “Social gan: Socially acceptable trajectories with generative adversarial networks,” in *Proceedings of the IEEE Conference on Computer Vision and Pattern Recognition*, 2018, pp. 2255–2264.
- [6] Namhoon Lee et al., “Desire: Distant future prediction in dynamic scenes with interacting agents,” in *Proceedings of the IEEE Conference on Computer Vision and Pattern Recognition (CVPR)*, July 2017.
- [7] Abdullah Mohamed et al., “Social-stgcnn: A social spatio-temporal graph convolutional neural network for human trajectory prediction,” in *Proceedings of the IEEE/CVF Conference on Computer Vision and Pattern Recognition (CVPR)*, June 2020.
- [8] Vineet Kosaraju et al., “Social-bigat: Multimodal trajectory forecasting using bicycle-gan and graph attention networks,” in *Advances in Neural Information Processing Systems*, 2019, pp. 137–146.
- [9] Dirk Helbing and Peter Molnar, “Social force model for pedestrian dynamics,” *Physical review E*, vol. 51, no. 5, pp. 4282, 1995.
- [10] Gianluca Antonini et al., “Discrete choice models of pedestrian walking behavior,” *Transportation Research Part B: Methodological*, vol. 40, no. 8, pp. 667–687, 2006.
- [11] C. G. Prevost et al., “Extended kalman filter for state estimation and trajectory prediction of a moving object detected by an unmanned aerial vehicle,” in *2007 American Control Conference*, 2007, pp. 1805–1810.
- [12] A. Alahi et al., “Social lstm: Human trajectory prediction in crowded spaces,” in *IEEE Conf. on Computer Vision and Pattern Recognition*, 2016.
- [13] Nachiket Deo and Mohan M Trivedi, “Convolutional social pooling for vehicle trajectory prediction,” in *Proceedings of the IEEE Conference on Computer Vision and Pattern Recognition Workshops*, 2018, pp. 1468–1476.
- [14] Mayank Bansal et al., “Chauffeurnet: Learning to drive by imitating the best and synthesizing the worst,” *Robotics Science and Systems (RSS)*, 2019.
- [15] Mariusz Bojarski et al., “End to end learning for self-driving cars,” *arXiv preprint arXiv:1604.07316*, 2016.
- [16] Rajesh Rajamani, *Vehicle dynamics and control*, Springer Science & Business Media, 2011.
- [17] Henggang Cui et al., “Deep kinematic models for physically realistic prediction of vehicle trajectories,” *arXiv preprint arXiv:1908.00219*, 2019.
- [18] Charles Richter et al., “Polynomial trajectory planning for aggressive quadrotor flight in dense indoor environments,” in *Robotics Research*, pp. 649–666. Springer, 2016.
- [19] Alexandr Andoni et al., “Learning polynomials with neural networks,” in *International conference on machine learning*, 2014, pp. 1908–1916.
- [20] Juan-Manuel Pérez-Rúa et al., “Learning how to be robust: Deep polynomial regression,” *arXiv preprint arXiv:1804.06504*, 2018.
- [21] Grigorios G Chrysos et al., “P-nets: Deep polynomial neural networks,” in *Proceedings of the IEEE/CVF Conference on Computer Vision and Pattern Recognition*, 2020, pp. 7325–7335.
- [22] Alex Graves, “Generating sequences with recurrent neural networks,” *CoRR*, vol. abs/1308.0850, 2013.
- [23] Junyoung Chung et al., “Empirical evaluation of gated recurrent neural networks on sequence modeling,” *arXiv preprint arXiv:1412.3555*, 2014.
- [24] Ashish Vaswani et al., “Attention is all you need,” in *Advances in neural information processing systems*, 2017, pp. 5998–6008.

- [25] J Bernardo et al., “Regression and classification using gaussian process priors,” *Bayesian statistics*, vol. 6, pp. 475, 1998.
- [26] Charlie Tang and Russ R Salakhutdinov, “Multiple futures prediction,” in *Advances in Neural Information Processing Systems*, 2019, pp. 15398–15408.